Gauche Propanal: Microwave Spectrum and Methyl Barrier

Jeremy Randell and A. Peter Cox

Department of Physical Chemistry, University of Bristol, BS8 1TH

H. Dreizler

Abteilung Chemische Physik im Institut für Physikalische Chemie der Universität Kiel

Z. Naturforsch. **42a**, 957–962 (1987); received July 11, 1987

The barrier hindering internal rotation of the methyl group was determined by analysing ground-state A, E splittings of rotational lines in the O_+ and O_- torsional states of *gauche* propanal. The value $V_3 = 886\ (10)\ cm^{-1}$ obtained can be compared with that obtained earlier for the *cis* rotamer.

The *A* rotational constant has also been determined, its value averaged over the two lowest states being 26248.41 (5) MHz.

Introduction

Propanal (propionaldehyde, CH_3CH_2CHO) exists in the gaseous phase as two rotational conformers; *cis* and *gauche* [1]. The barrier to internal rotation of the methyl group about the C – C bond has recently been determined from the ground state microwave spectrum for the *cis* conformer [2]. The purpose of the present paper is to report a value for the methyl barrier for the higher energy *gauche* form.

Previous microwave studies on the near-prolate *gauche* conformer had not identified either μ_b or μ_c type transitions, both predicted to be split by methyl rotation. Both sets are very dependent on the *A* rotational constant, and the μ_c transitions, being inversion type spectra, are split about the asymmetric rotor prediction by ± the torsional energy level splitting (ΔE). The best prediction of the *A* constant was accurate only to ± 500 MHz; this, combined with the unfavourable energy difference between the conformers (*gauche* – *cis* = $420(53)\ cm^{-1}$ [3]) has made assignment of weak *gauche* lines difficult in a complicated spectrum. The aim of the present work is to assign these cross-dipole transitions, principally to determine the methyl barrier but also to measure the *A* rotational constant.

Reprint requests to Dr. A. Peter Cox, Department of Physical Chemistry, University of Bristol, Bristol BS8 1TH, United Kingdom.

Experimental

Microwave spectra were studied at Bristol in the range 7 – 40 GHz using a conventional 100 kHz Stark modulated spectrometer with a three metre X-band stainless steel wave guide. Broad frequency scans were made in the region 18 – 40 GHz using backward wave oscillators, and accurate frequency measurements were made using klystrons with oscilloscope presentation. Measurements were made at dry ice temperatures with pressures in the range 1 – 7 Pa. Radiofrequency microwave double resonance (RFMDR) spectra were measured by the method of Wodarczyk and Wilson [4]. Radiofrequencies from 10 – 470 MHz were supplied by a Marconi TF801D signal generator and a Marconi TF2172 amplifier. The radiofrequency was square wave modulated at 100 kHz via a Hewlett Packard 1054A double balanced mixer. The splittings given in Table 3 were measured in Kiel using the very high resolution of a microwave Fourier transform spectrometer [5] in the region of 8 – 25 GHz, at – 60 °C and pressures down to 0.04 Pa.

Samples were purchased from Aldrich Chemical Co. Ltd. (Bristol) and Ega Chemie (Kiel).

Spectroscopic Analysis

The first step towards finding cross-dipole transitions was to obtain an improved prediction of the A rotational constant from structural calculations. This was done by using the extensive set of *cis* structural data [6] and rotating it into the expected

0932-0784 / 87 / 0900-0957 $ 01.30/0. – Please order a reprint rather than making your own copy.

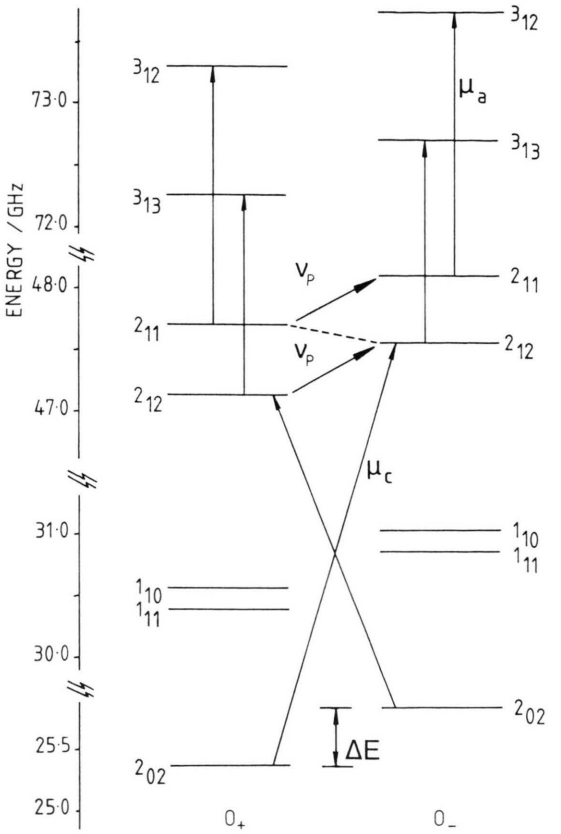

Fig. 1. The energy level diagram for the two lowerst torsional states of *gauche* CH_3CH_2CHO. *ΔE, the torsional energy level splitting, is 475.28(13) MHz;* ν_p represents the pump frequency of 419(1) MHz used to assign the μ_c-type transitions indicated.

gauche conformation, the parameters then being refined to fit the known B, C constants [7]. The procedure was checked using the nitrosoethane structures for which good *cis/gauche* information was available [3]. This suggested the accuracy of the calculations of A to be ± 200 MHz, thereby considerably narrowing the range of the spectroscopic search.

Even with the improved prediction it was not possible to identify the moderately weak adsorptions in a spectrum dominated by the *cis* conformer. It was decided therefore to employ the specificity of RFMDR to assign the spectra. Prediction using a coupled level Hamiltonian showed that the close degeneracy and strong mixing of the $(+)2_{11}$, $(-)2_{12}$ states (see Fig. 1) would allow the normally forbidden $(-)2_{11} \leftarrow (+)2_{11}$, $(-)2_{12} \leftarrow (+)2_{12}$ transitions to be used as r.f. pump transitions with μ_c-type lines as signal transitions. Figure 2 shows the use of μ_a type $3_{13} \leftarrow 2_{12}$ as signal transitions to optimise the spectrometer conditions; this result also shows that there is no possible doubt about the previous microwave assignments by Pickett and Scroggin [8]. For our convenience the spectra presented are from the oxygen-18 species which was studied concurrently. Using the same r.f. conditions, c-type $(+)2_{12} \leftarrow (-)2_{02}$, $(-)2_{12} \leftarrow (+)2_{02}$ transitions were identified as shown in Figure 3. On the basis of these two transitions, the whole series could be identified and measured under Stark conditions.

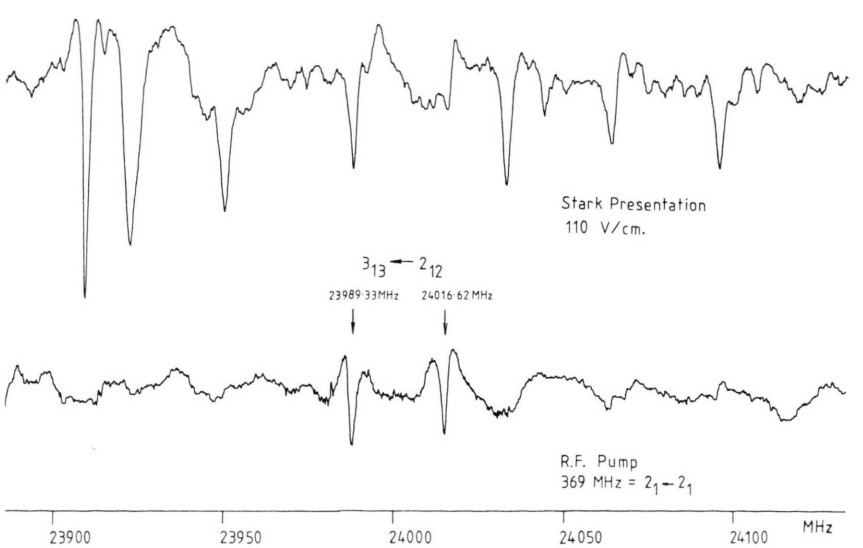

Fig. 2. Confirmation of the torsional energy level splitting in *gauche* $CH_3CH_2CH^{18}O$ using RFMDR. A similar experiment was used for the normal *gauche* species, see text.

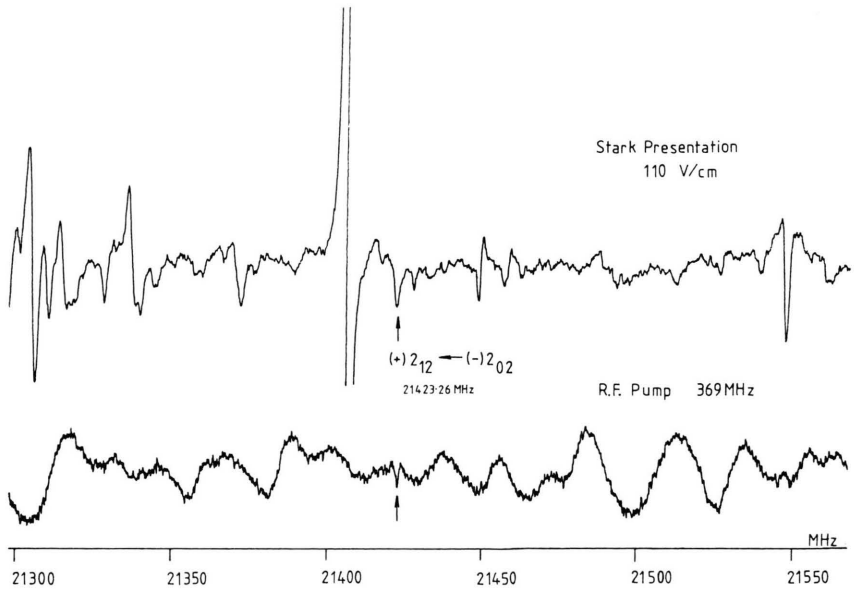

Fig. 3. Observation of c-type $(+)2_{12} \leftarrow (-)2_{02}$ transition of *gauche* $CH_3CH_2CH^{18}O$ under double resonance and Stark presentations. The r.f. resonance is clearly visible against the sinusoidal background.

The data were fitted to a version of Pickett's reduced axis system Hamiltonian including all quartic centrifugal distortion terms in Watson's A reduction [9]:

$$H = \begin{vmatrix} H_+ & H_\pm \\ H_\pm & H_- \end{vmatrix},$$

$$H_+ = A_+ P_A^2 + B_+ P_B^2 + C_+ P_C^2 + \text{quartic c.d.},$$

$$H_- = A_- P_A^2 + B_- P_B^2 + C_- P_C^2 + \text{quartic c.d.} + \Delta E,$$

$$H_\pm = [T_{BC} + T_j P^2](P_C P_B + P_B P_C).$$

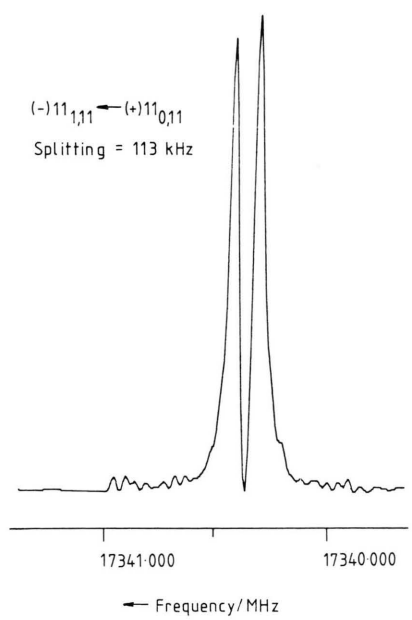

Fig. 4. $(-)11_{1,11} \leftarrow (+)11_{0,11}$ transition of *gauche* CH_3CH_2CHO showing the CH_3 A, E splitting. A section of 2 MHz out of a 25 MHz range of the power spectrum is given. Sample interval 20 ns, 640 K cycles. 1024 data points supplemented by 3072 zeros, pressure 0.04 Pa, temperature −60 °C.

Table 1 gives the centrifugal distortion analysis of all the measured lines. The parameters resulting from the least squares analysis are presented in Table 2.

The prediction for the methyl group internal rotation had shown the high J, c-type lines to have resolvable A, E, splittings, ~0.5 MHz. In fact no splittings were observed under Stark conditions indicating an even higher methyl barrier than expected. The splitting measurements were therefore undertaken at Kiel taking advantage of the higher resolution MWFT instrument. A typical A, E doublet can be seen in Figure 4. The splitting measurements were refined by a line-shape analysis. The barrier analysis was made with the internal axis method following the treatment of Woods [10]. The splittings and barrier calculations are present in Table 3. There are insufficient data to determine I_α and λ_A from the internal rotation fit, and these parameters have been taken from the structural determination. The CH_3 splittings have been adequately treated as being simply superim-

Table 1. Lines of *gauche* – CH_3CH_2CHO used for centrifugal distortion analysis. (OBS – CALC) derived using the constants of Table 2.

Upper level J K_a K_c	Lower level J K_a K_c	Obs*/MHz	(Obs-Calc)	Upper level J K_a K_c	Lower level J K_a K_c	Obs*/MHz	(Obs-Calc)
(−) 1 0 1	(−) 0 0 0	8462.92	−0.08	(+) 5 0 5	(+) 4 0 4	42290.40	−0.07
(+) 1 0 1	(+) 0 0 0	8462.92	0.20	(−) 5 1 5	(+) 5 0 5	21216.08	0.06
(+) 2 1 2	(−) 2 0 2	21289.07	0.10	(−) 5 0 5	(−) 4 0 4	42291.78	−0.07
(+) 2 0 2	(+) 1 0 1	16924.45	0.17	(+) 5 0 5	(−) 4 1 3	18921.21	0.10
(−) 2 1 2	(−) 1 1 1	16699.51	0.08	(−) 5 0 5	(+) 4 1 3	19853.63	0.10
(+) 2 1 1	(+) 1 1 0	17153.50	0.02	(+) 5 1 5	(−) 5 0 5	20278.25	0.01
(+) 2 1 2	(+) 1 1 1	16754.73	0.04	(−) 6 1 6	(+) 6 0 6	20727.41	0.03
(−) 2 1 2	(+) 1 1 0	17007.80	−0.06	(+) 6 1 6	(−) 6 0 6	19785.37	−0.06
(−) 2 0 2	(−) 1 0 1	16924.85	0.00	(−) 7 1 7	(+) 7 0 7	20168.41	−0.03
(−) 2 1 1	(−) 1 1 0	17097.45	−0.26	(+) 7 1 7	(−) 7 0 7	19221.84	0.01
(−) 2 1 1	(+) 2 1 1	419.00**	0.51	(−) 8 1 8	(+) 8 0 8	19544.66	0.01
(−) 2 1 2	(+) 2 1 2	419.00**	−0.26	(+) 8 1 8	(−) 8 0 8	18592.82	0.03
(+) 2 1 1	(−) 1 1 1	16845.17	0.11	(−) 9 1 9	(+) 9 0 9	18861.95	−0.17
(−) 3 1 3	(−) 2 1 2	25161.15	0.09	(+) 10 1 9	(+) 10 0 10	27218.97	0.05
(+) 3 1 3	(−) 3 0 3	21033.63	0.00	(+) 11 1 11	(−) 11 0 11	16376.87	0.00
(+) 3 1 2	(−) 2 1 2	25761.95	−0.07	(−) 11 1 11	(+) 11 0 11	17348.42	−0.04
(+) 3 1 2	(+) 2 1 1	25616.22	−0.17	(−) 12 1 12	(+) 12 0 12	16532.59	0.00
(−) 3 0 3	(−) 2 0 2	25384.41	0.03	(+) 12 1 12	(−) 12 0 12	15552.92	−0.06
(−) 3 1 2	(−) 2 1 1	25647.73	0.13	(−) 12 1 11	(−) 12 0 12	29570.32	0.02
(+) 3 2 1	(+) 2 2 0	25396.02	−0.04	(+) 13 1 13	(−) 13 0 13	14699.90	−0.01
(+) 3 0 3	(+) 2 0 2	25383.61	−0.08	(−) 13 1 13	(+) 13 0 13	15688.33	0.01
(−) 3 2 2	(−) 2 2 1	25392.89	−0.17	(−) 14 1 14	(+) 14 0 14	14824.25	0.05
(+) 3 2 2	(+) 2 2 1	25392.33	−0.08	(+) 14 1 14	(−) 14 0 14	13826.20	0.03
(−) 3 2 1	(−) 2 2 0	25396.58	−0.03	(+) 15 1 15	(−) 15 0 15	12940.39	−0.05
(−) 3 1 3	(+) 2 1 1	25015.50	0.07	(+) 16 1 16	(−) 16 0 16	12051.27	−0.01
(+) 3 1 3	(+) 2 1 2	25129.17	0.13	(−) 16 1 16	(+) 16 0 16	13071.34	0.10
(+) 4 0 4	(+) 3 0 3	33839.36	0.05	(+) 17 1 17	(−) 17 0 17	11167.03	−0.03
(+) 4 1 3	(+) 3 1 2	34192.73	−0.14	(+) 18 1 18	(−) 18 0 18	10295.60	0.01
(−) 4 0 4	(−) 3 0 3	33840.42	−0.01	(−) 18 1 18	(+) 18 0 18	11341.28	0.00
(+) 4 2 3	(+) 3 2 2	33855.41	0.00	(+) 19 1 19	(−) 19 0 19	9444.19	0.02
(−) 4 1 4	(+) 4 0 4	21629.49	0.10	(−) 19 1 19	(+) 19 0 19	10504.26	0.05
(−) 4 1 3	(−) 3 1 2	34196.21	0.09	(−) 20 1 20	(+) 20 0 20	9694.48	−0.09
(−) 4 2 3	(−) 3 2 2	33856.44	0.10	(+) 20 1 20	(−) 20 0 20	8619.12	−0.07
(−) 4 1 4	(−) 3 1 3	33506.64	−0.17	(−) 21 1 21	(+) 21 0 21	8917.92	−0.01
(+) 4 1 4	(+) 3 1 3	33502.34	−0.08	(−) 22 1 22	(+) 22 0 22	8178.79	0.07

* Observations corrected for A, E splitting where observed.

** R.f. pump frequency, included in the fit.

Table 2. *Gauche* CH_3CH_2CHO: Average (±) rotational constants (MHz), distortion constants (kHz)* and torsional constants. Errors are 1σ from the fit.

	$\frac{O_+ + O_-}{2}$		$\frac{O_+ - O_-}{2}$
A	26248.4079 ± 0.050		1.8726 ± 0.090
B	4314.7255 ± 0.009		−0.0134 ± 0.005
C	4148.1596 ± 0.008		−0.1288 ± 0.003
Δ_J	3.754 ± 1.0		−0.231 ± 0.07
Δ_{JK}	−175.729 ± 4.4		−3.490 ± 1.60
Δ_K	176.766 ± 3.4		2.906 ± 1.65
δ_K	92.379 ± 0.4		3.095 ± 0.70
		ΔE	475.278 ± 0.13 MHz
		T_{BC}	23.760 ± 0.02 MHz
		T_j	6.524 ± 1.88 kHz

* Watson's A reduction (II^r representation).

posed upon the ± splittings arising from internal rotation about the C – CHO bond. This procedure gives a satisfactory fit (see Table 3) and probably cannot be improved within the rigid top-rigid frame single degree of freedom model.

Discussion

Molecules undergoing methyl internal rotation about a C – C ($sp^3 - sp^3$) bond may be considered as substituted ethanes (see Table 4). In this context it is interesting to compare the methyl barrier of *gauche* propanal, determined in this work, with the *cis* conformer [2] and the isoelectronic molecules but-1-ene [10] and nitrosoethane [3], see Figure 5.

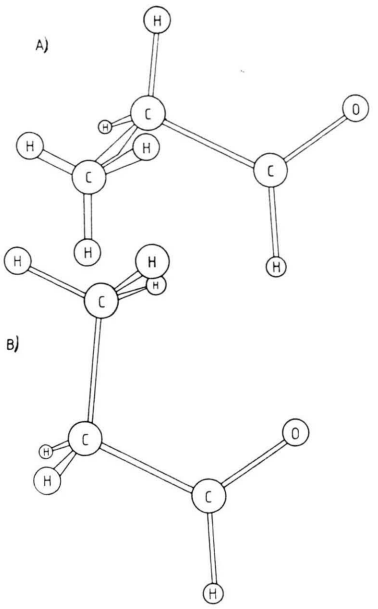

Fig. 5. Conformations of A) *gauche* propanal, B) *cis* propanal.

Table 3. MWFT splitting measurements and methyl barrier parameters for *gauche* CH_3CH_2CHO (*not included in the fit).

Upper level			Lower level			Splitting	(Obs-Calc)
J	K_a	K_c	J	K_a	K_c	kHz	kHz
(−) 4	1	4	(+) 4	0	4	170*	−18
(−) 5	1	5	(+) 5	0	5	176	−5
(−) 7	1	7	(+) 7	0	7	159	−4
(−) 8	1	8	(+) 8	0	8	157	5
(−) 9	1	9	(+) 9	0	9	145	4
(−) 10	1	10	(+) 10	0	10	135	6
(−) 11	1	11	(+) 11	0	11	113	−3
(−) 12	1	12	(+) 12	0	12	102	−1
(+) 3	2	1	(+) 2	2	0	782*	55
(+) 3	2	2	(+) 2	2	1	761*	16
(−) 3	2	1	(−) 2	2	0	757*	30
(−) 3	2	2	(−) 2	2	1	746*	1

Δ_0 −5.632(70) MHz
S 65.46(81)
I_α 3.16 uÅ^2

λ_A 0.7885
λ_B 0.5889
F 180.3 GHz
V_3 886(10) cm^{-1}

The barriers for both propanal conformers are lower than for ethane probably due to an attractive mechanism involving the oxygen atom. This is illustrated by the *cis* conformer, where the interaction of the proton at the barrier position and the oxygen atom lowers the V_3 barrier significantly with respect to the parent ethane molecule. For nitrosoethane a similar trend would be expected, however in this case the *cis* and *gauche* methyl barriers are remarkably similar ($\sim$904 cm^{-1}) suggesting that the lone pair of electrons on nitrogen play an additional rôle. Both but-1-ene V_3 barriers are higher than for ethane, this being expected the presence of the bulky, $-CHCH_2$, substituent. In *cis* but-1-ene the vinylic hydrogen-methyl hydrogen interaction increases the methyl barrier by $\sim$300 cm^{-1} with respect to ethane.

In general, the methyl barriers for the substituted ethanes appear closely related to the parent molecule, bearing in mind the errors involved, i.e. the single degree-of-freedom model neglecting V_6 and contributions from other vibrations. Rotation of the molecules from *gauche* to *cis* alters the V_3 barrier in such a way that it can be explained by invoking simple repulsive and attractive interactions.

Acknowledgements

One of us (Jeremy Randell) thanks S.E.R.C. for a research studentship. H. Dreizler thanks the Deutsche Forschungsgemeinschaft and the Fonds der Chemie for funds.

[1] S. S. Butcher and E. B. Wilson jr., J. Chem. Phys. **40**, 1671 (1964).
[2] J. A. Hardy, A. P. Cox, E. Fliege, and H. Dreizler, Z. Naturforsch. **37a**, 1035 (1982).
[3] J. A. Hardy, Ph. D. Thesis, University of Bristol, 1980.

Table 4. Methyl group, V_3, barriers for comparison with *cis* and *gauche* propanal. All barriers correspond to I_α = 3.16 uÅ^2 (* c.f. [2] V_3 = 794(3) cm^{-1}, I_α = 3.03 uÅ^2).

Name	Formula	Methyl barrier		Ref.
		cis V_3/cm^{-1}	*gauche* V_3/cm^{-1}	
Propanal	CH_3CH_2-CHO	768(8)*	886(10)	this work
But-1-ene	$CH_3CH_2-CHCH_2$	1396(4)	1105(14)	[11]
Nitrosoethane	CH_3CH_2-NO	902(14)	905(2)	[3]
Ethane	CH_3CD_2-H	1007(1)		[12, 13]

[4] F. J. Wodarczyk and E. B. Wilson jr., J. Mol. Spectrosc. **37,** 445 (1971).
[5] G. Bestmann, H. Dreizler, H. Mäder, and U. Andresen, Z. Naturforsch. **35a**, 392 (1980); G. Bestmann and H. Dreizler, Z. Naturforsch. **37a,** 58 (1982); W. Stahl, G. Bestmann, H. Dreizler, U. Andresen, and R. Schwarz, Rev. Sci. Instrum. **56,** 1759 (1985).
[6] J. Randell, A. P. Cox, K. W. Hillig II, Misako Imachi, M. S. La Barge, and R. L. Kuczkowski, to be published.
[7] C. M. P. Brown, B. Sc. Thesis, University of Bristol, 1985.
[8] H. M. Pickett and D. G. Scroggin, J. Chem. Phys. **61,** 3954 (1974).
[9] L. Halonen and P. H. Turner, Private Communication.
[10] R. C. Woods, J. Mol. Spectrosc. **21,** 4 (1966).
[11] S. K. Kondo, E. Hirota, and Y. Morino, J. Mol. Spectrosc. **28,** 471 (1968).
[12] E. Hirota, S. Saito, and Y. Endo, J. Chem. Phys. **71**(3) 1183 (1979).
[13] E. Hirota, Y. Endo, S. Saito, and J. L. Duncan, J. Mol. Spectrosc. **89,** 285 (1981).